AUTONOMOUS CRACK HEALING PERFORMANCE IN CONCRETE MONITORED BY DIGITAL IMAGE CORRELATION AND ACOUSTIC EMISSION TECHNIQUES

Kyoto University Regular Member ○ Takahiro Nishida, Chien-wen Huang, Tomoki Shiotani, Hisafumi Asaue
Vrije Universiteit Brussel Tsangouri Eleni

1. INTRODUCTION

In this study, the four stages of bending test were conducted on lab-scale reinforced concrete specimens carrying autonomous healing agent in order to investigate autonomous crack healing performance in concrete. The initial loading was provided to initiate the crack formation as well as healing agent breakage. After the healing agent was released and filled the crack void, reloading of the specimens is performed. As the fracture damage occurs, the Digital Image Correlation (DIC) technique and Acoustic Emission (AE) were carried out to visualize the displacement and strain field formed during fracture before and after healing activation and monitors the internal damage of concrete loses its accuracy as damage extends, respectively. The main results are compared with imaging of concrete defects and repair after healing in terms of DIC and AET techniques.

2. MATERIALS AND METHODS

2.1 Mixtures and autonomous healing materials

An ordinary Portland cement was used in all mixtures. The details of mixture proportions used in the experimental program were are given is Table 1. A polyurethane-based autonomous healing agent was used for crack repair. This polymerization of polyurethane stars foaming and expanding in humidity exposure atmosphere. During the preparation of the concrete beam, 18 tubular capsules were embedded below and above steel bars. A controlled vibration was used for the compaction of the rectangular specimen. During curing, the specimen was placed again in the air-conditioned room for at least 8 days and was covered with wet cloths until the date of experiment.

Table 1. Mixtures proportions of concretes

Component	Portland Cement	Water	Sand	Gravels	Additive AE	Agent water
Volume	668(kg/m^3)	336(kg/m^3)	790(kg/m^3)	1029(kg/m^3)	6,344(g/m^3)	840.9(g/m^3)

2.2 Three Point Flexural Test

The specimen with 400 mm in length, 100 mm in width and 100 mm in height was subjected to a three-point bending test under displacement control condition. The specimens were placed on supporting bins. The loading force was applied in the middle by means loading pin. The designed crack width was increased with a velocity of 3mm/ min until a width of 3mm was reached. Once the desired width condition had been achieved, the experiment was terminated, and the beam was unloaded. After autonomous crack repair, beams were reloaded until an additional crack width of 3mm was reached.

2.3 Digital Image Correlation (DIC) Technique

This technique was carried out to monitor the micro cracks propagation with sub-pixel opening and track the micro cracks between consecutive digital images taken during the deformation. The high speed camera system is attached on a tripod and face the speckled pattern are (240x100mm) at the notched middle area of the beam. The focused and calculated DIC camera setup captured images every 5 seconds during testing.

2.4 Acoustic Emission and Acoustic Emission Tomography (AET) technique

AET technique considers travel time tomography algorithms and provides an imaging of concrete defects and repair after

Keywords: Autonomous healing material, Digital Image Correlation, Acoustic Emission Tomography
Contact address: C3-b4S16, Katsura Campus, Kyoto University, Nishikyo, Kyoto 615-8530, Japan, Tel: +81-75-383-3496

healing [4]. During three point bending test, specimens were instrumented with an AE system. When the concrete beams were loaded, elastic waves are emitted due to the crack formation. These waves were detected by AE sensors which attached to the surface of the beam. In this study, 12 sensors resonant at 60 kHz were coupled to the specimen by using a hot-glue materials and captured elastic waves arriving at the surface of beam with amplitude higher than 50dB (AE Threshold). The parameters of waveform such as sample rate, pre-trigger and length are 1MPSP, 128 and 1k, respectively.

3. EXPERIMENTAL RESULTS

Fig. 1 shows crack opening observed by DIC techniques.After being subjected to 1st cycle bending test, the specimen expectedly make internal fractures spreadly. Three cracks were visible by using DIC (Fig.1 (a)). After 12 hour healing activation, specimen was carried out the cycle 2 experiment and captured the images by DIC. It was found that three cracks were healed (Fig.1 (b)). Furthermore, in Fig.1(c) and Fig.1 (e), after 2nd and 3rd cycle bending test, the existed crack openings spread and tiny crack reopened. However, DIC results of each initial stage show that the cracks were healed effectively by autonomous healing materials as shown in Fig.1 (d) and Fig (f). This may be because specimen cracked inside, the capsules break opened, the autonomous healing materials wicked out, and then simply filled the voids. This should be noted that the capsules can only heal cracks or defects once, if the cracks reopen, it cannot be healed twice.

Fig. 2 shows velocity distribution measured by AET technique after 4 cycle bending test. After undergoing 1st cycle bending test, the wave speed changed in defective region (Fig. 2(a)). However, After 12 hour healing activation, the damaged position has higher wave speed (Fig. 2(b)), which corresponds to the autonomous healing location of the specimen (Open red square). A shown in Fig. 1(g) and Fig.2 (g), as autonomous healing materials has no more effect on specimen after first time healing, crack opening has seriously propagated and wave speed changed in defective region became more significant than other area in the specimen.

4. CONCLUSIONS

In this paper, two advance monitoring techniques have been applied to observe the efficiency of autonomous crack healing on concrete. Good agreement between the visual examination results and the corresponding tendency for the wave speed changed is evident, indicating that autonomous healing materials has significant effect in concrete specimen and the effect may ceased after the first time healing.

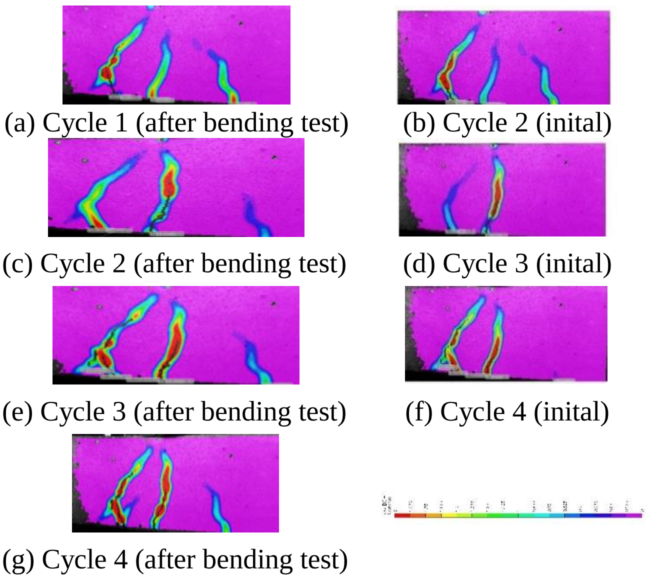

(a) Cycle 1 (after bending test) (b) Cycle 2 (inital)
(c) Cycle 2 (after bending test) (d) Cycle 3 (inital)
(e) Cycle 3 (after bending test) (f) Cycle 4 (inital)
(g) Cycle 4 (after bending test)

Fig.1 Crack opening observed by DIC technique

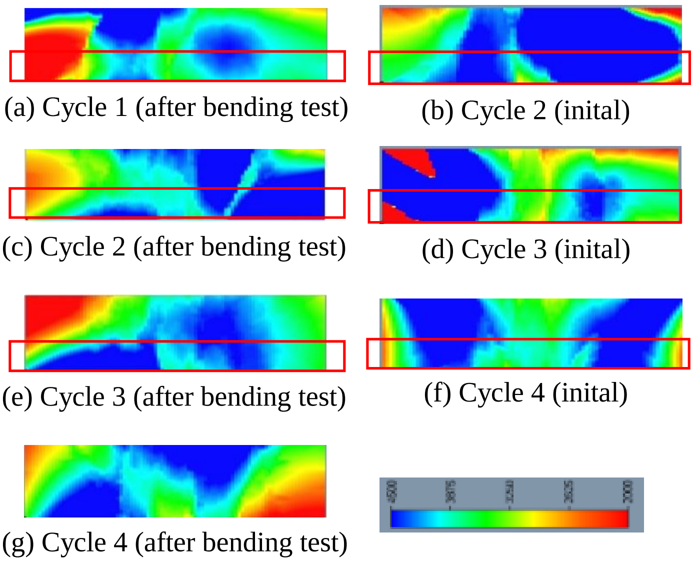

(a) Cycle 1 (after bending test) (b) Cycle 2 (inital)
(c) Cycle 2 (after bending test) (d) Cycle 3 (inital)
(e) Cycle 3 (after bending test) (f) Cycle 4 (inital)
(g) Cycle 4 (after bending test)

Fig. 2 Velocity distribution measured by AET technique

REFERENCES

T. Shiotani, S. Osawa, S. Momoki and H. Ohtsu, "Visualization of damage in RC bridge deck for bullet trains with AE tomography," Springer, Advances in Acoustic Emission Technology, 2014, pp. 357-368.